Hindawi
Security and Communication Networks
Volume 2022, Article ID 9791417, 1 page
https://doi.org/10.1155/2022/9791417

Retraction

Retracted: Water Quality Substance Detection System Based on Internet of Things

Security and Communication Networks

Received 10 November 2022; Accepted 10 November 2022; Published 27 November 2022

Copyright © 2022 Security and Communication Networks. This is an open access article distributed under the Creative Commons Attribution License, which permits unrestricted use, distribution, and reproduction in any medium, provided the original work is properly cited.

Security and Communication Networks has retracted the article titled "Water Quality Substance Detection System Based on Internet of Things" [1] due to concerns that the peer review process has been compromised.

Following an investigation conducted by the Hindawi Research Integrity team [2], significant concerns were identified with the peer reviewers assigned to this article; the investigation has concluded that the peer review process was compromised. We therefore can no longer trust the peer review process, and the article is being retracted with the agreement of the Chief Editor.

References

[1] J. Zhang, "Water Quality Substance Detection System Based on Internet of Things," *Security and Communication Networks*, vol. 2022, Article ID 2815078, 11 pages, 2022.

[2] L. Ferguson, "Advancing Research Integrity Collaboratively and with Vigour", 2022, https://www.hindawi.com/post/advancing-research-integrity-collaboratively-and-vigour/.

Hindawi
Security and Communication Networks
Volume 2022, Article ID 2815078, 11 pages
https://doi.org/10.1155/2022/2815078

WILEY | Hindawi

RETRACTED

Research Article

Water Quality Substance Detection System Based on Internet of Things

Jing Zhang

Office of Educational Administration, Tangshan Normal University, Tangshan 063000, Hebei, China

Correspondence should be addressed to Jing Zhang; zhangjing@tstc.edu.cn

Received 6 May 2022; Revised 13 June 2022; Accepted 16 June 2022; Published 8 August 2022

Academic Editor: Mohammad Ayoub Khan

Copyright © 2022 Jing Zhang. This is an open access article distributed under the Creative Commons Attribution License, which permits unrestricted use, distribution, and reproduction in any medium, provided the original work is properly cited.

According to the sources of pollution in different river regions, the characteristics of rivers and lakes, and on the basis of investigation and analysis of the actual situation of water environment monitoring in different river regions, this paper carries out a research on the optimization of water quality detection and gives the definition of a super network as a super network based on a hypergraph structure. Moreover, according to the simulation results of topological parameters, this paper analyzes the structural characteristics of the super network and combines the Internet of Things technology to construct a water quality material detection system. In addition, this paper evaluates the water quality detection effect of the system proposed in this paper through a control experiment. According to the quality inspection results, it can be seen that the accuracy rate of the water quality material detection system based on the Internet of Things proposed in this paper is more than 92%, which verifies that the system model proposed in this paper has a good effect.

1. Introduction

Automatic detection of water environment has begun to flourish and has begun to be put into use on a large scale in developed countries such as Europe, the United States, and Japan. There are various types of water quality monitoring instruments abroad, including monitoring instruments, monitoring boxes, and portable water quality monitoring terminals that can quickly monitor. The first two devices are used for early water quality monitoring, and the latter is now widely used in developed countries such as Europe and the United States. At present, foreign monitoring instruments such as temperature, pH value, and CO_2 concentration are relatively mature. The monitoring instruments designed in Europe and the United States and other countries have huge advantages in terms of volume and weight, and the monitoring speed is relatively fast, the operation is simple, the practicability is strong, and the energy consumption is less, and the advantages are obvious. However, the structure of foreign monitoring instruments and equipment is relatively complex, it is difficult to adapt to China's water environment monitoring system, and the price is very expensive, so it is not the primary choice for monitoring the water environment in China.

At present, the monitoring objects, monitoring items, and monitoring methods for rivers and lakes are too uniform and monotonous. Moreover, the monitoring points are mainly concentrated in the national-controlled and provincial-controlled sections, and the total control and management system is not yet perfect, which cannot fully adapt to the changes in pollutants with different characteristics in each region and the requirements for water environment safety in the basin. Therefore, it is necessary to establish a spatiotemporal database of watershed water quality management information, a watershed water quality information management system, and a visualization platform, to form an efficient and practical monitoring technology and basic theoretical system for the watershed, and to provide an integrated technical system and basic theoretical support for the security of the watershed water environment. At the same time, it is necessary to select typical areas for engineering demonstration on the basis of technical optimization integration and development.

In this paper, the Internet of Things technology is used to construct a water quality material detection system, and the real-time monitoring of water quality material content is carried out through intelligent methods to improve the effect of water quality detection and management.

2. Related Work

The water quality monitoring vehicle is equipped with various small- and medium-sized instruments and analyzers, which can analyze and measure a number of water quality indicators. In fact, it is a small mobile laboratory [1]. The method of laboratory testing has disadvantages such as high-operational threshold and strong lag, which is not conducive to the promotion and popularization of technology. With the development of semiconductor technology, water quality testing instruments with water quality sensors as the core have become the first choice for water quality testing technology due to their portability and real-time performance. Portable water quality analysis instruments have the advantages of timely detection, small size, convenient operation, and easy operation [2]. The import price of high-end water quality monitoring instruments is expensive. Most of these products are agents of well-known foreign companies, and their products are only used in a few large-scale key projects [3]. Generally, small- and medium-scale farmers cannot afford their high purchase and cost. Maintenance Costs

At present, the research of water quality information monitoring system mainly focuses on three aspects: water quality information collection, water quality information transmission, and water quality information feedback. First of all, in terms of water quality information collection, sensor technology and electronic technology are mainly used to convert water quality indicators such as dissolved oxygen, pH, water temperature, salinity, and other water quality parameters into corresponding electrical signals, and then digitalize the water quality indicators through analog-to-digital conversion. Provide data support for subsequent monitoring and processing. Compared with the previous experience and laboratory analysis of water samples, a variety of high-precision water quality parameter acquisition sensors are used to collect water quality data accurately and efficiently, which can greatly improve the real-time monitoring level of water quality parameters [4].

In terms of water quality information feedback, it mainly refers to the automatic control algorithm of the research equipment, which is processed and analyzed according to the data obtained by the breeding monitoring system, so as to realize the prediction and early warning of water quality parameters, and automatically control the aerators, feeders, operation of alarms, and other equipment. The control strategy adopted at the beginning is the most direct control idea. The measured water quality index content is compared with the preset threshold value. If the actual value is lower than the lower limit, the aerator will be turned on, and if it reaches the upper limit, the aerator will be turned off [5]. Literature [6] applies fuzzy PID to the control of dissolved oxygen, improves the traditional PID control, and designs a cascade control system, which is composed of a universe fuzzy PID controller, and aerator speed PID regulator to achieve more for rational and scientific regulation. Literature [7] proposed an adaptive control algorithm, and the dissolved oxygen content was stable at 4 mg/L~6 mg/L. The application of neural network to the prediction and early warning of water quality parameters has become a hotspot of current research.

The gray system prediction method is suitable for systems with poor information, and GM(1,1) and its improved models have been used in water quality prediction. Literature [8] establishes a mathematical model with the help of multiobjective programming model and GM(1,1) prediction method, and the purpose is to realize the optimal allocation scheme of water resources and maximize the social and ecological benefits. The model established with the gray forecasting method can predict the future water supply and water consumption of the city well according to the relevant data, but the accuracy of the forecasting method is not clear. Literature [9] used the gray prediction model to analyze the accuracy of the model based on real-time monitoring data, using the posterior difference method, but this method could not solve the error problem.

Combined forecasting is to combine multiple forecasting methods, such as neural network, time series algorithm, deep learning algorithm, moving window algorithm, reinforcement-learning algorithm, to combine several of them to form a new forecasting method, which is unique to decentralized single forecasting algorithm through combined model. In order to improve the accuracy of model predictions, the overall uncertainty and instability can be reduced. Literature [10] proposed a model combining fuzzy neural network and gray. The model is used to predict the changes of water quality parameters in each water area, and then the obtained water quality parameter prediction values are fused by the T-S fuzzy neural network method, which makes the obtained prediction values more accurate and establishes a trend model of the predicted values. The parameters vary within a reasonable range. Literature [11] continued to study the gray network model and improved the model, that is, to integrate it with the neural network, use one-dimensional sequence to obtain three sets of predicted values through the improved gray model, and then use these three sets of predicted values as the neural network. Input takes the initial data as the output of the neural network and obtains the ideal neural network model after continuous learning and training. The improved gray neural network is a combined model obtained by combining the two. The model combines the advantages of both, the model is widely used, and its application in the prediction of water quality parameters can improve the accuracy. Literature [12] introduced the artificial bee colony (ABC) algorithm. Due to the long learning time of the traditional BP neural network, it will cause a local minimum problem. The solution process of each layer of the BP neural network can be transformed into a process for bees to find the best nectar source. This transformation proposes a new BP network model (ABC-BP).

The traditional monitoring and measurement methods of water environment cannot solve the requirements of

RETRACTED

monitoring and measurement of water environment in the whole country. The detection system is also not perfect usually; single-point monitoring, lack of connection between monitoring points, unable to adapt to the changes of different characteristic pollutants in different regions, unable to respond to changes in the water environment of river water bodies in time, and unable to provide real-time water pollution prediction, and early warning are some of the shortcomings [13]. For the needs of pollution control and management, the existing water environment monitoring points are far from being able to meet, especially in the border areas of provinces, countries, and areas with many pollution disputes, which need to be further optimized [14]. In view of the fact that different methods of modern detection are usually carried out together, and the monitoring network needs to occupy a large area and requires high water quality, it is necessary to establish a multi-data fusion transmission, multi-database platform sharing, data model simulation and evaluation [15].

3. IoT-Based Hypernetwork Algorithm

3.1. IoT-Based Hypernetwork Foundation. Hypergraphs can be classified into various types according to the directions and weights of edges in the hypergraph. The hypernetwork model studied in this paper belongs to the undirected and unweighted hypergraph, and a hypernetwork model is represented by an association matrix $C = (c_{ij})_{MxN}$. Among them, c_{ij} is an element in C, M is the number of hyper-edges of the hypernetwork, and N is the number of nodes of the hypernetwork. When some topological parameters of the super network are calculated, the adjacency matrix A needs to be used, and the adjacency matrix A can be obtained according to the correlation matrix C. Since there are N nodes in the undirected hypernetwork, its adjacency matrix is a square matrix of order N, that is $A = (a_{ij})_{NxN}$. Among them, a_{ij} is an element in A that represents the number of hyperedges containing node i and node j.

A hypergraph is defined as follows: there is a finite set $X = \{x_1, x_2, \ldots, x_n\}$, if the following conditions are met:

(1) $E_i \neq \varnothing\ (i = 1, 2, \ldots, m)$

(2) $\cup_{i=1}^{m} E_i = X$

Then, the binary relation $H =$ (X, E) is called a hypergraph. Among them, the element $x_1, x_2, ..., x_n$ of the set X represents the nodes of the hypergraph, the set E is the set of edges of the hypergraph, and each element $E_i = \left\{v_{i_1}, v_{i_2}, \ldots, v_{i_j}\right\}\ (1 \le j \le n)$ is called a hyperedge of the hypergraph. Figure 1 shows a hypergraph H. Among them, there is node V = {vl, v2, v3, v4, v5, v6, v7, v8}, hyperedge set E = {el, e2, e3, e4, e5}. Among them, there is el = {vl, v2}, e2 = {v2,3, v4},e3 = {v3, v6, v7,e4 = {v4, v5, v8},e5 = {v6, v8}.

The hypernetwork definition can be described as follows: we assume that $\Omega = \{(X, E)|(X, E)\}$ is a finite hypergraph and G is a mapping from [0, +oo) to Ω. For any given $t \ge 0$, $\Omega = \{X(t), E(t)\}$ is a finite hypergraph and $N^*(t)$ represents the total number of times the hypergraph has changed by time 1. If $\{N^*(t), t \ge 0\}$ is a random process,

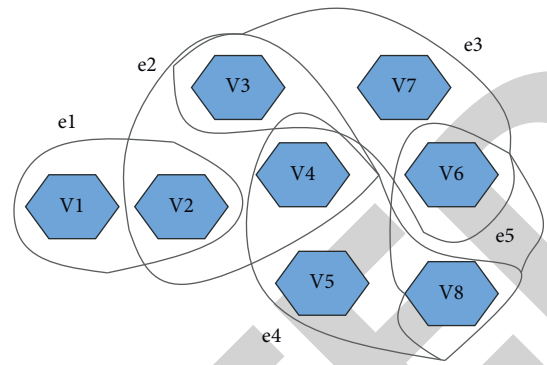

Figure 1: Hypergraph H.

for a sufficiently large time t, we call $G = (X(t), E(t))$ a hypernetwork.

The hypergraph association matrix is defined as follows: we assume that the binary relation $H = (X, E)$ is a hypergraph. If matrix C satisfies the following conditions:

(1) Each row of C is related to the node of H;

(2) Each column of C is related to the edge of H;

(3) If node i is included in edge j, then there is $C_{ij} = 1$;

Then, the matrix C is said to be the correlation matrix of the hypergraph H. For example, the H correlation matrix C in Figure 1 is

$$C = \begin{pmatrix} 1 & 0 & 0 & 0 & 0 \\ 1 & 1 & 0 & 0 & 0 \\ 0 & 1 & 1 & 0 & 0 \\ 0 & 1 & 0 & 1 & 0 \\ 0 & 0 & 0 & 1 & 0 \\ 0 & 0 & 1 & 0 & 1 \\ 0 & 0 & 1 & 0 & 0 \\ 0 & 0 & 0 & 1 & 1 \end{pmatrix}. \quad (1)$$

The hypergraph adjacency matrix can be described as follows:

We assume that the binary relation H=(X,E) is a hypergraph. If matrix A satisfies the following conditions:

(1) Each row of A is related to the node of H.

(2) Each column of A is related to the node of H.

(3) Element ay in matrix A represents the number of hyperedges including node i and node j. When there is $i = j$, there is $a_{ij} = 0$. Then, the matrix A is said to be an adjacency matrix of the hypergraph H. For example, the adjacency matrix of the hypergraph H in Figure 1 is

RETRACTED

$$A = \begin{pmatrix} 0 & 1 & 0 & 0 & 0 & 0 & 0 & 0 \\ 1 & 0 & 1 & 1 & 0 & 0 & 0 & 0 \\ 0 & 1 & 0 & 1 & 0 & 1 & 1 & 0 \\ 0 & 1 & 1 & 0 & 1 & 0 & 0 & 1 \\ 0 & 0 & 0 & 1 & 0 & 0 & 0 & 1 \\ 0 & 0 & 1 & 0 & 0 & 0 & 1 & 1 \\ 0 & 0 & 1 & 0 & 0 & 1 & 0 & 0 \\ 0 & 0 & 0 & 1 & 0 & 0 & 1 & 0 \end{pmatrix}. \quad (2)$$

According to the definition of the association matrix and the adjacency matrix, the two matrices can be transformed into each other. When the correlation matrix C of the hypernetwork is known, the adjacency matrix A can be obtained by the following formula.

$$A = CC^T - D. \quad (3)$$

In the above formula, C^T is the transpose matrix of C. D is a diagonal matrix in which the elements of the main diagonal are the degrees of each node in H.

The relevant properties of the hypergraph are the following:

(1) Cut set: We set V_1 and V_2 to be two node sets, which belong to the two disconnected branches left after removing the set from G, then the edge set E connecting V_1 and V_2 is called a cut set.

(2) Subhypergraph: The set $J \in \{1,2, ..., m\}$ is given, and $H_{(V,J)} = (E_j; j \in J)$ is called a partial hypergraph generated by the set J. A set $A \in V$ is given, and $H_{(A,E)} = (E_j \cap A: 1 \le j \le m, E_j \cap A \ne \varnothing)$ is a sub-hypergraph of H derived from node set A. Both partial hypergraphs and sub-hypergraphs derived from node set A are special cases of subgraphs of H. In general, $J = \{1, 2, \ldots, m\}$ and $A \subset V$ are given, and $H_{(A,J)} = (E_j \cap A: j \in J, E_j \cap A \ne \varnothing)$ is called the subhypergraph derived from node sets A and J.

3.2. Topological Metrics for Hypernetworks. The study of the hyperdegree distribution of nodes will help to explore the properties of hypernetworks. In a hypernetwork H, the hyperdegree D of a node j is defined as the number of hyperedges that contain this node. We set the association matrix $C = (c_{ij})_{MxN}$ of H, then the hyperdegree of node j is

$$D_j = \sum_{i=1}^{m} c_{ij}. \quad (4)$$

In formula (14), c_{ij} is an element of the correlation matrix C. If node j is included in hyperedge i, then there is $c_{ij} = 1$; otherwise, there is cy = 0. When the hyperdegree distribution of the node is studied, the calculation formula of the distribution probability $P(D_j)$ of the hyperdegree D is

$$P(D_j) = \frac{N_j}{N}. \quad (5)$$

Among them, N_j represents the number of points with hyperdegree D_j, and N is the total number of nodes in the hypernetwork.

In this paper, when the degree of a node is calculated, the nodes inside the hyperedge are fully connected by default. For the degree of a node, the definition in hypernetworks and complex networks is the same, that is, the degree k of a node i represents the number of nodes directly adjacent to i. We set the adjacency matrix $A = (a_{ij})_{NxN}$ of H, then the degree k_i of node i is

$$\begin{aligned} k_i &= \sum_{j=1}^{n} a_{ij} \\ &= \sum_{j=1}^{n} a_{ji}. \end{aligned} \quad (6)$$

The calculation of the degree of each node is to analyze the degree distribution of the node. The calculation formula of the degree distribution probability $P(k_i)$ is as follows:

$$P(k_i) = \frac{N_i}{N}. \quad (7)$$

Among them, N_i represents the number of nodes with hyperdegree k_i, and N is the total number of nodes of H.

The average clustering coefficient refers to the average probability that a hyperedge is interconnected between two neighbor nodes connected to the same node in a hypernetwork. This parameter is an important parameter for judging whether the hypernetwork satisfies the small-world characteristics, and it is usually used to describe the density of hypertriangles in the hypernetwork, that is, the larger the clustering coefficient, the greater the density of hyper-triangles. The formula for calculating the clustering coefficient is

$$C_2(H) = \frac{\sum_{s=1}^{n} \lambda_s^3 - 6t}{\sum_{s=1}^{n} \left(\left(\sum_{i=1}^{n} u_{is} \right)^2 - 1 \right) \lambda_s^2 - 6t}. \quad (8)$$

Among them, λ_s is the eigenvalue of the adjacency matrix A, and $U = (u_{ij})$ is an orthogonal matrix, in which each column represents the eigenvector corresponding to λ_s, and these eigenvectors constitute an orthonormal basis of the N-dimensional Euclidean space. The parameter t represents the number of pseudohypertriangles in the hypernetwork. In a hypernetwork, a hypertriangle is defined as a closed sequence consisting of three distinct nodes and three distinct hyperedges, which can be represented as v_i, E_p, v_j, E_q, v_k, E_r, v_i. Among them, three nodes are adjacent to each other, as shown in Figure 2. A closed sequence that does not satisfy the above conditions is called a pseudohypertriangle. The calculation formula of t is given in the literature. That is

$$t = \sum_{j=1}^{m} (-1)^{j+1} a_j. \quad (9)$$

In formula (9), a represents the number of pseudohypertriangles in the intersection of j hyperedges, and its

RETRACTED

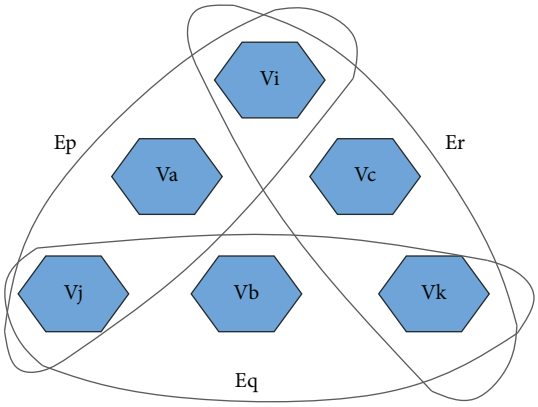

Figure 2: Schematic diagram of a super triangle.

calculation formula is $a_j = \sum_{i_1,i_2,\ldots,i_k} \binom{\alpha_{i_1,i_2,\ldots,i_k}}{3}$, and $\alpha_{i_1,i_2,\ldots,i_k}$ represents the number of nodes in the intersection of hyperedge set $\{E_{i_1}, E_{i_2}, \ldots, E_{i_k}\}$.

In biological networks, this formula is called transfer clustering, and the specific form of the formula is

$$C_2(H) = \frac{6 * \text{Super triangle number}}{\text{The number of path length is 2}}. \quad (10)$$

Among them, the hypertriangles are multiplied by 6 in the numerator of this expression because each hypertriangle contributes 6 paths of length 2, and it is guaranteed to be $C_2(H) = 1$ in the complete graph K_n.

Figure 3 is an example graph of a competition hypernetwork, among them, nodes represent species and hyperedges represent groups of species competing for the same food. By observing Figure 3, we can see that there are only two hypertriangles in the hypernetwork, which are composed of nodes v_2, v_4, v_{10} and v_2, v_4, v_{10} respectively, and the corresponding hypertriangle sequences are v_2, E_2, v_4, E_3, v_{10}, E_1, v_2 and v_2, E_2, v_5, E_3, v_{10}, E_1, v_2. The number of paths of length 2 in this hypernetwork is 48. Formula (10) is used to know the average clustering coefficient $C_2(H) = 6 * (2/48) = 0.25$ of the hypernetwork, which indicates that there are 14 triples among the 18 triplet nodes that join at least two different competition groups to join three different competition groups, in other words, the hypertriangle density of this hypernetwork is 0.25.

In a hypernetwork, the distance d from node i to node j refers to the number of hyperedges on the shortest path connecting nodes i and j, that is, the minimum distance from node i to node j. Also, the average path length of a hypernetwork refers to the average distance between any two nodes i and j, which is denoted by L. When the average path length is calculated, a distance matrix of the hypernetwork needs to be constructed to store the path values between nodes. This matrix is a square matrix of order N. If the distance matrix $D = (d_{ij})_{NxN}$ of the super network H is set, the calculation formula of the average path length is

$$L = \frac{2}{N(N-1)} \sum d_{ij}. \quad (11)$$

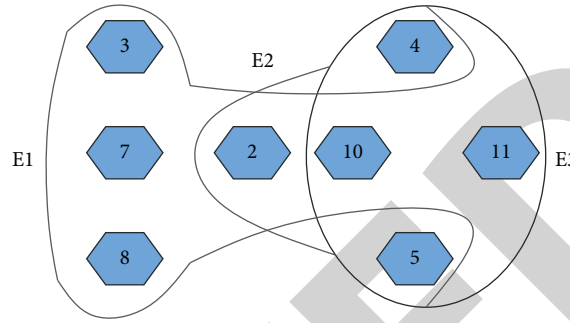

Figure 3: Competitive hypernetwork diagram.

Among them, there is $i \geq j$, and N is the total number of nodes in the network. If the hypernetwork nodes i and j belong to different connected branches, there is no shortest path between these two nodes, and the distance d_{ij} between the two points is equal to infinity.

In hypernetworks, subgraph centrality parameters are analyzed, which are very important to study the characteristics of real-world networks and identify key nodes of the network. The subgraph centrality of a node refers to the sum of closed paths of different lengths from and to the node. Since closed paths can be divided into trivial closed walks and nontrivial closed walks, all cyclic and acyclic subgraphs must be considered when calculating subgraph centrality parameters. The calculation formula of node i subgraph centrality is [16]:

$$C_{SH}(i) = \sum_{j=1}^{N} \left(u_{ij}\right)^2 e^{\lambda_j}. \quad (12)$$

In formula (12), λ_j is the eigenvalue of the adjacency matrix A in the super network H, $U = (u_{ij})_{NxN}$ is an orthogonal matrix, and it satisfies that each column is the eigenvector corresponding to the eigenvalue λ_j, and these vectors constitute the N-dimensional Euclidean an orthonormal basis of space. After the value of the subgraph centrality of each node is calculated, the subgraph centrality of the super network can be obtained by calculating the average value. In literature [17], the formula for calculating the centrality of the hypernetwork subgraph is

$$\begin{aligned} \langle C_{SH} \rangle &= \frac{\sum_{i=1}^{N} C_{SH}(i)}{N} \\ &= \frac{\sum_{i=1}^{N} e^{\lambda_i}}{N}. \end{aligned} \quad (13)$$

It can be seen from formula (13) that the subgraph centrality of the super network is related to the network size N and the eigenvalue of the adjacency matrix A.

Many concepts in hypergraphs are generalized from network science, engineering, and psychology, and the entropy metric is one of them. It is an important indicator reflecting the heterogeneity of network structure. Hypergraph entropy is defined as follows:

RETRACTED

$$I(H) = -\sum_{i=1}^{n} \lambda_i lo_2 \lambda_i. \tag{14}$$

Among them, λ_i is the eigenvalue of matrix $L(H)$, and its calculation formula is

$$\lambda_i = \frac{u_i}{\sum_{x \in V} D(x)}. \tag{15}$$

In formula (15), the eigenvalue u_i is obtained by calculating the Laplacian matrix L of the hypernetwork H. Because the sum of all eigenvalues u is the same as the cumulative sum of the elements on the main diagonal of the matrix. Therefore, for any $i \in \{1, 2, \ldots, n\}$, there are $0 \le \lambda_i \le 1$ and $\sum_{i=1} \lambda_i = 1$. According to the above content, the solution process of the entropy index can be described as follows: first, according to the adjacency matrix A of the hypernetwork, the diagonal matrix $D = \text{diag}(D(x_1), D(x_2), \ldots, D(x_n))$ is obtained. Then, formula $L(\text{H}) = \text{D-A(H)}$ is used to solve the Laplacian matrix L(H) of the hypernetwork and the eigenvalues u, of the matrix. Since the adjacency matrix A(H) in the hypernetwork H is a positive real matrix, L(H) is a positive semidefinite matrix with the smallest eigenvalue $u_0 = 0$. Finally, according to formulas (15) and (14), the entropy I(H) of the Wei and super network is obtained.

3.3. Classical Models of Hypernetworks and Complex Networks. The WS small-world network model can study the characteristics of the network when the value of P ranges from 0 to 1. In this network, when $N \gg K \gg \ln(N) \gg 1$, then $L(0) \approx (N/2K)$ and $C(0) \approx (3/4)$, and when P is close to 1, then $L \approx L_{\text{random}} \approx (\ln(N)/\ln(K))$ and $C \approx C_{\text{random}} \approx (K/N) \ll 1$. Furthermore, the probability P exists in a range such that $L(p)$ and L_{random} are almost as small in this range. However, when $C(p) \gg C_{\text{random}}$, by randomly reconnecting several edges, the value of L(p) can be decreased to form a small-world network.

Figure 4 shows the degree distribution of the WS small-world network under different probabilities P, where the number of nodes in the network is $N = 1000$ and $K = 6$. It is not difficult to find from the figure that the trend of each curve satisfies the characteristics of Poisson distribution, and these curves reach the maximum value when the degree value is equal to 5 or 6. In addition, as the probability P increases, the maximum value of the curve decreases and the distribution range increases.

For the study of the small world model, in addition to the abovementioned WS small world model, there is another kind of small world model construction algorithm, which is called the NW small world model. The construction algorithm of the NW small world model is as follows:

3.3.1. Start with a Rule Graph. Initially, it is given a ring-nearest-neighbor coupled network, which contains N nodes, and each node is connected to its left and right K/2 nodes, where K is an even number.

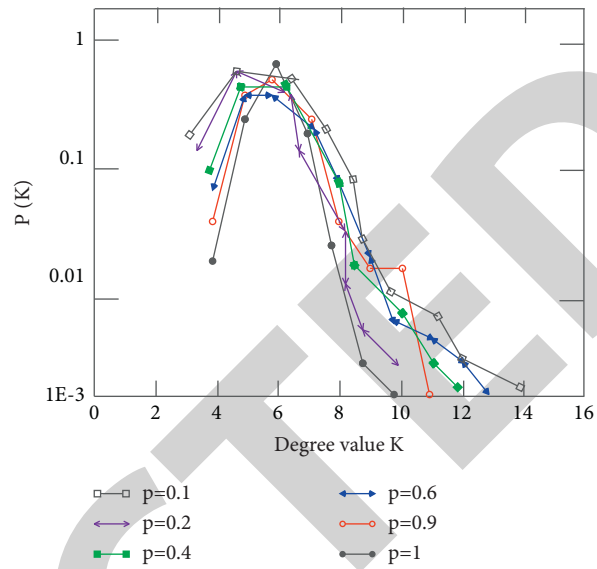

Figure 4: Degree distribution of WS small world network.

3.3.2. Randomly Add Edges. On the basis of the original network, the operation of adding random edges is performed, that is, new edges are added to the NK/2 pairs of nodes in the network randomly according to the probability P. It is stipulated that after the random edge addition process ends, the original network must not have multiple edges and self-loops.

Figure 5 depicts the degree distribution of the NW model under different P values, where $N = 1000$ and $K = 6$. It is not difficult to see from the figure that with the continuous increase of P, the range of the degree distribution is also getting larger, but the maximum value is getting smaller and smaller. The reason is that the NW model is based on the "random edge addition" mechanism, which ensures that the degree of each node is at least K, and the degree distribution curve of the network is affected by the number S of long-range edges in the NW model. In addition, the degree distribution of the NW model obeys the Poisson distribution with mean K_p, and its function is

$$P(s) = e^{-Kp} \frac{(Kp)^s}{s!}. \tag{16}$$

The degree of nodes in the BA network constructed based on the growth mechanism and the preferential connection mechanism has no obvious characteristic length, so it is called a scale-free network. The construction algorithm of the BA scale free network is described as follows:

(1) Growth. It gives an initial network, and when starting from a network with m_0 nodes, each time a new node is added and connected to m existing nodes, and $m \le m_0$.

(2) Priority connection. The probability $\prod_i$ that the newly added node is connected to the existing node v_i is proportional to the degree k_i of the node v_i, namely:

RETRACTED

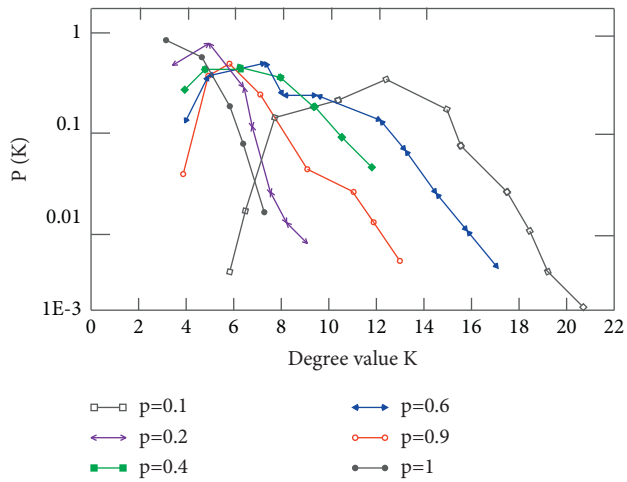

Figure 5: Degree distribution of NW small-world network.

$$\prod_i = \frac{k_i}{\sum_j k_j}. \tag{17}$$

Among them, the numerator is the degree of the node and the denominator $\sum_j k_j$ is the sum of the degrees of all nodes present in the network. After t steps, the number of nodes in the network is $N = t + m_0$ and the number of edges is $mt + m_0$. m_0 represents the number of edges present in the initial network.

It is concluded that the degree distribution of the scale-free network model obeys a power-law distribution, which can be approximated by a power function as follows:

$$p(k) \propto 2m^2 k^{-3}. \tag{18}$$

With the continuous enrichment and improvement of hypergraph theory, more and more scholars use hypergraph structure to study the characteristics of real networks, and build many hypergraph models.

The hypernetwork model will provide an important reference for future research on the evolutionary model of hypernetwork. The construction algorithm of the super network evolution model is as follows:

(1) Initial conditions. The model builds an initial network. The network has m_0 initial nodes and a hyperedge containing these nodes. Then, we perform the following two steps:

(2) Hyperedge growth. In each time step, m new nodes are added to the existing hypernetwork, and a node is selected in the network to form a new hyperedge with m new nodes.

(3) Hyperdegree priority connection. m new nodes are connected to a node of an existing hypernetwork. If the probability $\prod_i (d_H(i))$ is assumed to represent the probability that the hyperedge is connected to the old node i, then this probability depends on the hyperdegree $d_H(i)$ of node i, that is,

$$\prod_i (d_H(i)) = \frac{d_H(i)}{\sum_{j \in N} d_H(i)}. \tag{19}$$

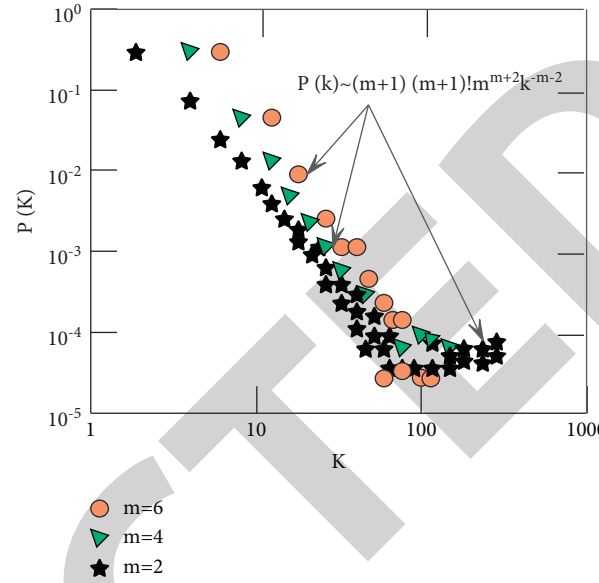

Figure 6: Degree distribution of the super network model.

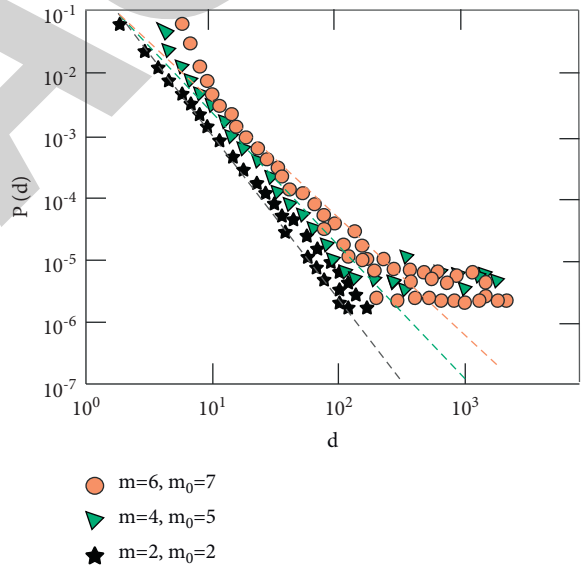

Figure 7: Degree distribution of the evolution model of the hypernetwork.

After t time steps, the number of nodes in it is $mt + m_0$ and the number of hyperedges is $t + 1$. Since the nodes inside the hyperedge are fully connected, the number of edges between nodes is $((m_0(m_0 - 1) + tm(m - 1))/2)$.

According to the method of the main equation, the results of hyperdegree and degree are analyzed, and it is concluded that the hyperdegree distribution can be approximated by a power function as follows:

$$p(d_H) \propto (m + 1)(m + 1)! d_H^{-m-2}. \tag{20}$$

The degree distribution can be approximated by a power function as follows:

RETRACTED

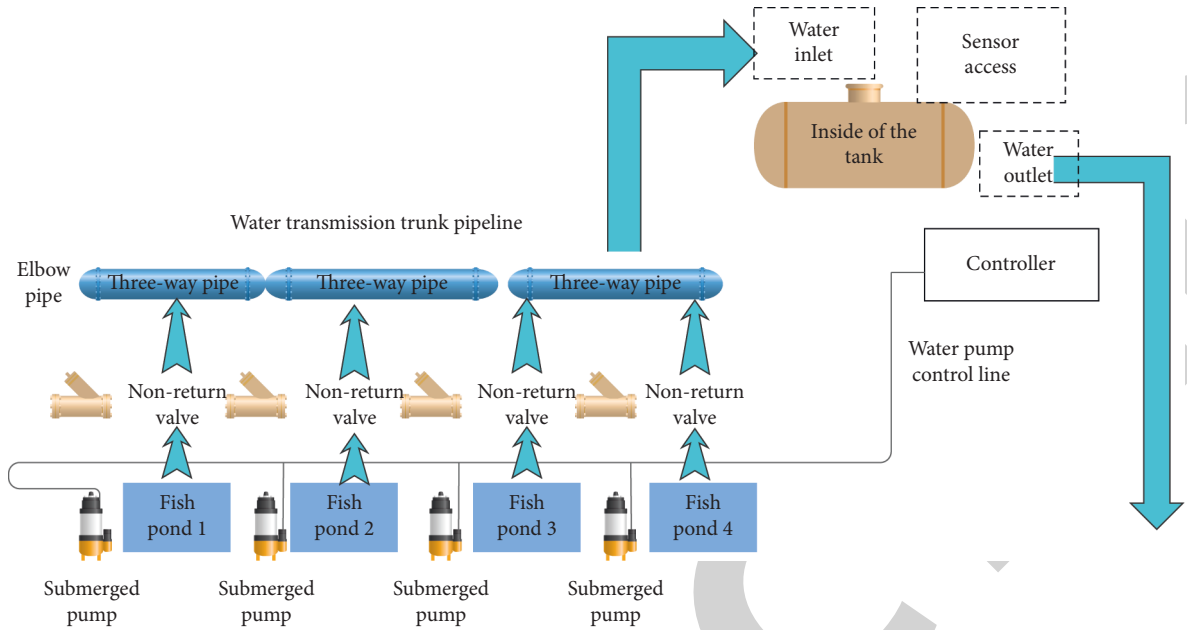

Figure 8: Schematic diagram of water sample collection.

$$p(k) \propto (m+2)(m+2)!m^{m+2}k^{-m-2}. \quad (21)$$

The degree distribution of the hypernetwork model is shown in Figure 6. Using the related theory and properties of hypergraphs, another kind of construction algorithm of hypernetwork evolutionary model is proposed. According to the construction algorithm, only one new node is added in each time step, and this node is combined with multiple existing nodes in the original network to form a new hyperedge. The specific construction algorithm of the hypernetwork evolution model is as follows:

(1) *Initialization*. Initially, the hypernetwork has m_0 nodes $v_1, v_2, \ldots, v_{m_0}$, and a hyperedge $E = \{v_1, v_2, \ldots, v_{m_0}\}$ contains these m_0 nodes.

(2) *Hyperedge growth*. In each time interval t, a new node v is added, which is combined with the existing m ($m \leq$ mo) nodes in the super network to generate a new super edge.

(3) *Priority connection*. According to the hyperdegree first connection mechanism, the new node selects the existing m nodes in the network to combine to generate hyperedges. That is, the probability $\prod(d_H(i))$ of selecting the connected node i each time is equal to the ratio of the hyperdegree $d_H(i)$ of the node i to the sum of the hyperdegree $d_H(j)$ of the existing node j in the hypernetwork, namely:

$$\prod(d_H(i)) = \frac{d_H(i)}{\sum_j d_H(j)}. \quad (22)$$

Among them, $d_H(i)$ is equal to the number of hyperedges containing node i. After time t, the hypernetwork will contain $t+1$ hyperedges, $m_0 + t$ nodes, and the sum of the hyperdegrees of all nodes is $m_0 + t(m+1)$.

Figure 7 shows the degree distribution of nodes when the number of nodes is 10000, $m0 = 3,5,7$ and $m = 2,4,6$. It is not difficult to find from Figure 6 that the degree distribution of the model obeys the power-law distribution, indicating that the hypernetwork has scale-free characteristics. The hyperdegree distribution of the nodes in the hypernetwork also obeys the power law distribution, which can be approximated by the power function of the power exponent $\gamma = 2 + (1/m)$. By analyzing the power exponent of hyperdegree, the value range of this exponent is (2, 3). In addition, when $m = 1$, the γ-value is the power exponent of the BA scale-free network.

4. The Water Quality Material Detection System Based on the Internet of Things

The function of the water sample collection part is to collect water samples at different collection points and to transport the water from each water source to the central water tank. This part is mainly the design of the pumping pipeline. The main pumping pipeline for water sample collection is composed of polyvinylchloride (PVC) pipes, as shown in Figure 8.

The system can be divided into two parts. The first is a data processing server module with Netty as the core. Its main functions are submodules for data reception, data sticking, and subpacket processing, data storage and abnormal message push. The second is to use SpringBoot as the back-end framework and Vue as the back-end management module developed by the front-end framework. It mainly includes the display of water quality data, the visualization of data and the management of water quality collection equipment. The overall architecture of the whole system is shown in Figure 9.

RETRACTED

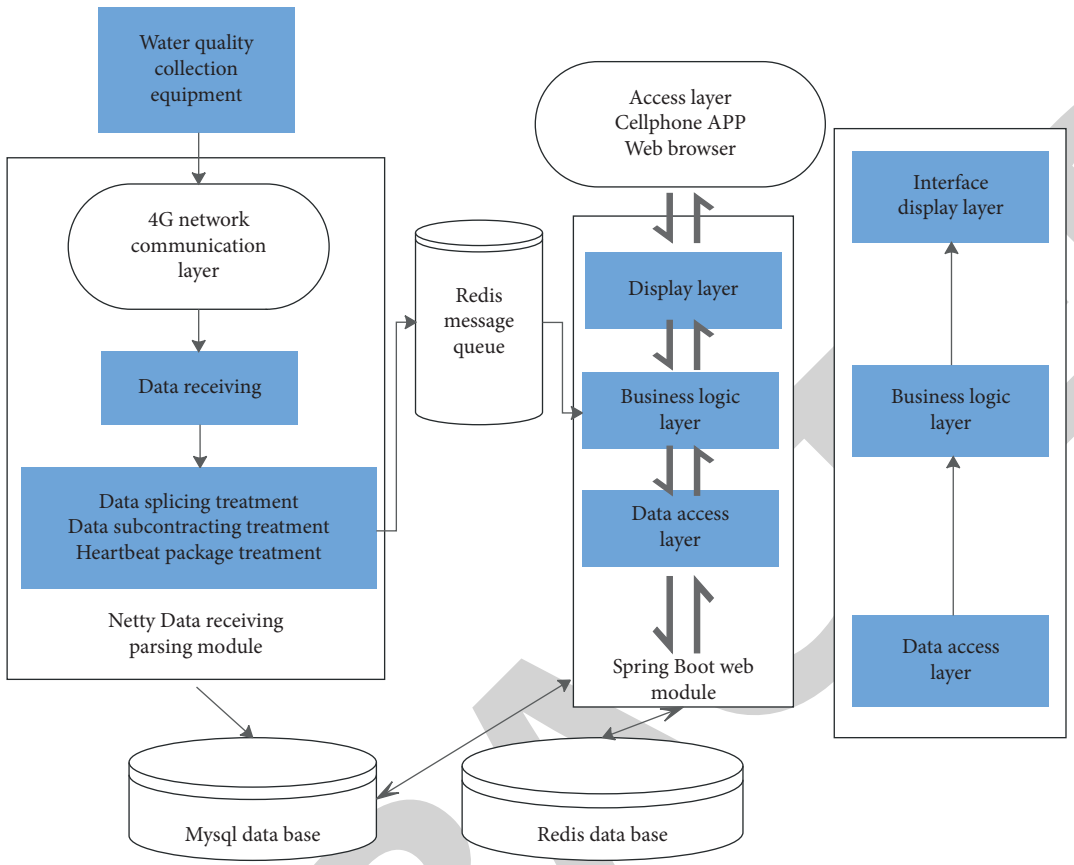

Figure 9: Overall architecture of the system.

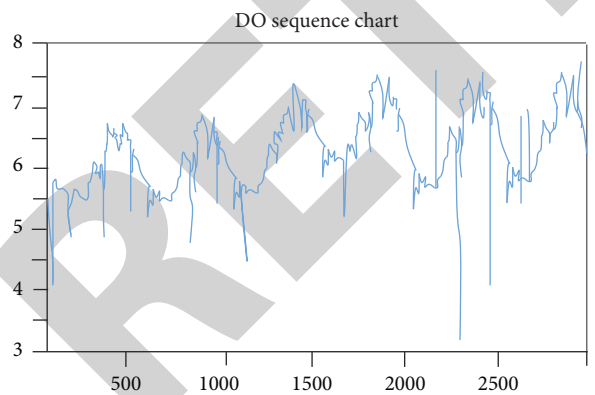

Figure 10: Timing diagram of raw data.

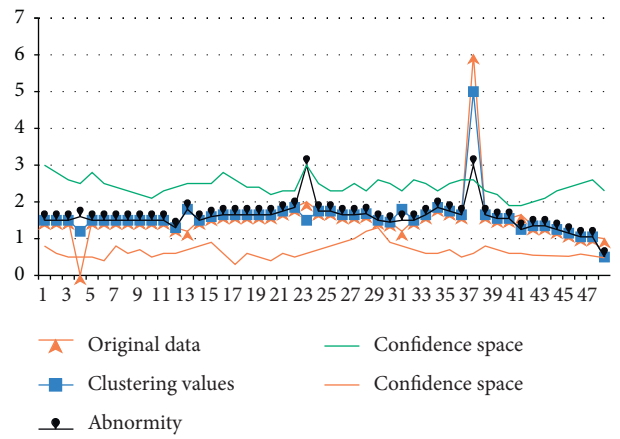

Figure 11: Result diagram of anomaly detection.

This paper combines the actual situation of "Construction and Application Demonstration of Aquatic Products Traceability and Safety Early Warning Platform Based on Internet of Things Technology" to detect abnormal water quality parameters. The monitoring frequency of data is once every three minutes, that is, a set of training original sequences is obtained as shown in Figure 10.

It can be seen from Figure 10 that the given time series data set has a periodic law, and the overall trend of the curve is stable and changes within a stable range. However, there are also some apparently suspicious "abnormal" point information, as shown in Figure 11.

On the basis of the above research, the effectiveness of the water quality material detection system based on the Internet of Things proposed in this paper is verified, and the detection results are compared with the standard results, and the detection accuracy is calculated. The results are shown in Table 1.

RETRACTED

Table 1: Statistical table of the accuracy of water quality detection of the water quality material detection system based on the Internet of Things.

Num	Water quality testing
1	94.45
2	95.18
3	92.44
4	95.86
5	94.45
6	92.22
7	93.74
8	92.16
9	94.59
10	93.32
11	94.16
12	93.71
13	92.88
14	95.13
15	92.29
16	94.49
17	93.10
18	93.75
19	93.93
20	94.33
21	93.84
22	95.73
23	92.74
24	93.47
25	92.36
26	95.95
27	94.63
28	92.64
29	95.48
30	93.08
31	95.06
32	95.23
33	94.92
34	95.98
35	92.28
36	92.88

From the above water quality testing results, the water quality detection system based on the Internet of Things proposed in this paper has an accuracy rate of more than 92% for water quality detection, which verifies that the system model proposed in this paper has a good effect.

5. Conclusion

The continuous acceleration of industrialization has made the problem of water basin pollution more and more unavoidable, and the environmental pollution has become more and more alarming. These problems are mainly reflected in these aspects: the total discharge of water pollutants and dirty water in the country is still very large, the severity of pollution is still at a very serious level, and the water quality in many places is still getting worse and worse. At the same time, the step-by-step deterioration of the ecosystem has not been effectively suppressed, and the environment is also becoming harsh. This paper combines the Internet of Things technology to build a water quality material detection system, uses an intelligent method to monitor the content of water quality materials in real time, and evaluates the water quality detection effect of the system proposed in this paper through a control experiment. According to the quality inspection results, it can be seen that the accuracy rate of the water quality material detection system based on the Internet of Things proposed in this paper is more than 92%, which verifies that the system model proposed in this paper has a good effect.

Data Availability

The data that support the findings of this study are available from the corresponding author upon reasonable request.

Conflicts of Interest

The author declares no potential conflict of interests with respect to the research, authorship, and/or publication of this article.

Acknowledgments

This work was supported by the Scientific Research Fund Project of Tangshan Normal University, Project Name: Research and implementation of water quality substance detection system based on Internet of things (project number: 2022C58).

References

[1] D. Chao, J. Chen, Q. Dong, W. Wu, D. Qi, and S. Dong, "Ultrastable and ultrasensitive pH-switchable carbon dots with high quantum yield for water quality identification, glucose detection, and two starch-based solid-state fluorescence materials," *Nano Research*, vol. 13, no. 11, pp. 3012–3018, 2020.

[2] J. P. Bakhoum, N. A. Diop, E. H. T. Bodian et al., "Development of an on-site early warning water quality monitoring system for pesticide detection by absorption and photo-induced fluorescence," *Environmental Science and Pollution Research*, vol. 27, no. 36, Article ID 45238, 2020.

[3] D. Chao, J. Chen, Q. Dong, W. Wu, D. Qi, and S. Dong, "Ultrastable and ultrasensitive pH-switchable carbon dots with high quantum yield for water quality identification, glucose detection, and two starch-based solid-state fluorescence materials," *Nano Research*, vol. 13, no. 11, pp. 3012–3018, 2020.

[4] S. Pandiarajan, S. Thambiratnam, and I. R. B. Sivaruban, "Biomonitoring and detection of water quality using Ephemeroptera, plecoptera and Trichoptera (EPT) complex in karanthamalai stream of eastern ghats," *Indian Journal of Ecology*, vol. 46, no. 4, pp. 818–822, 2019.

[5] S. Rathi, "S-PLACE GA for optimal water quality sensor locations in water distribution network for dual purpose: regular monitoring and early contamination detection - a software tool for academia and practitioner," *Water Supply*, vol. 21, no. 2, pp. 615–634, 2021.

[6] S. C. Ballen, G. M. Ostrowski, J. Steffens, and C. Steffens, "Graphene oxide/urease nanobiosensor applied for cadmium detection in river water," *IEEE Sensors Journal*, vol. 21, no. 8, pp. 9626–9633, 2021.

RETRACTED

[7] A. K. Tshamala, M. K. Musala, G. K. Kalenga, and H. D. W. MumapandaMumapanda, "Assessment of surface water quality in kakanda: detection of pollution from mining activities," *Journal of Environmental Protection*, vol. 12, no. 9, pp. 561–570, 2021.

[8] G. F. Santonastaso, A. Di Nardo, E. Creaco, D. Musmarra, and R. Greco, "Comparison of topological, empirical and optimization-based approaches for locating quality detection points in water distribution networks," *Environmental Science and Pollution Research*, vol. 28, no. 26, Article ID 33844, 2021.

[9] R. Mabvouna Biguioh, S. B. B. Adogaye, P. M. Pete et al., "Microbiological quality of water sources in the West region of Cameroon: quantitative detection of total coliforms using Micro Biological Survey method," *BMC Public Health*, vol. 20, no. 1, pp. 346-347, 2020.

[10] M. Jongman, P. C. Carmichael, and M. Bill, "Technological advances in phytopathogen detection and metagenome profiling techniques," *Current Microbiology*, vol. 77, no. 4, pp. 675–681, 2020.

[11] F. Bayat, T. F. Didar, and Z. Hosseinidoust, "Emerging investigator series: bacteriophages as nano engineering tools for quality monitoring and pathogen detection in water and wastewater," *Environmental Sciences: Nano*, vol. 8, no. 2, pp. 367–389, 2021.

[12] A. M. Motlagh and Z. Yang, "Detection and occurrence of indicator organisms and pathogens," *Water Environment Research*, vol. 91, no. 10, pp. 1402–1408, 2019.

[13] M. Kitajima, H. P. Sassi, and J. R. Torrey, "Pepper mild mottle virus as a water quality indicator," *NPJ Clean Water*, vol. 1, no. 1, pp. 19–9, 2018.

[14] H. Song, Y. Zhou, Z. Li et al., "Inner filter effect between upconversion nanoparticles and Fe(ii)-1,10-phenanthroline complex for the detection of Sn(ii) and ascorbic acid (AA)," *RSC Advances*, vol. 11, no. 28, Article ID 17212, 2021.

[15] J. Peng, C. Q. Xia, Y. Xu et al., "Crystallization of CsPbBr3 single crystals in water for X-ray detection," *Nature Communications*, vol. 12, no. 1, pp. 1531–1610, 2021.

[16] S. Mani Tripathi and S. Chaurasia, "Detection of Chromium in surface and groundwater and its bio-absorption using biowastes and vermiculite," *Engineering Science and Technology, an International Journal*, vol. 23, no. 5, pp. 1153–1161, 2020.

[17] M. Domańska, K. Hamal, B. Jasionowski, and J. Łomotowski, "Bacteriological contamination detection in water and wastewater samples using OD600," *Polish Journal of Environmental Studies*, vol. 28, no. 6, pp. 4503–4509, 2019.

RETRACTED